

The Use of Contrast-Enhancement Cardiovascular Magnetic Resonance Imaging in Cardiomyopathies

Marlon A.G.M. Olimulder, Michel A. Galjee, Jan van Es,
Lodewijk J. Wagenaar and Clemens von Birgelen
*Medisch Spectrum Twente
The Netherlands*

1. Introduction

The clinical applications of cardiovascular magnetic resonance imaging (CMR), are expanding as the result of the development in hardware, pulse sequence and the ability of post-processing techniques. As the result of the flexibility of CMR to use different pulse-sequences, with or without the use of Gadolinium, CMR has developed as a powerful tool for clinical relevant tissue characterization. CMR in combination with the contrast-enhancement (CE) technique was initially developed to distinguish viable from non-viable myocardium following myocardial infarction. Nowadays, CE-CMR is increasingly used for tissue characterization in ischemic as well as non-ischemic cardiomyopathies to determine the exact etiology, guide proper treatment, and predict outcome and prognosis. In this chapter, we would like to discuss and illustrate the value of CE-CMR imaging in various cardiomyopathies.

2. Utility of different CMR acquisition modes in cardiomyopathy

CMR imaging includes several techniques that can be used in various combinations to assess left ventricular functional parameters, morphology, as well as myocardial disorders (such as edema, scar/fibrosis, microvascular obstruction, myocardial salvage) within one examination. Therefore, it is increasingly used in clinical practice for the diagnosis and management of cardiac diseases. In this respect, recent reviews concerning this aspect have been published (Marcu et al., 2007; Olimulder et al. 2011; Vogel-Claussen et al. 2006; Vohringer 2007; Weinsaft et al. 2007). Some technical aspect of cine - and CE imaging but also T2-weighted imaging (increasingly used when CE imaging is applied) are shortly discussed below.

2.1 Cine CMR for quantitative assessment of ventricular dimension, function and mass

By application of ECG-gated, breath-holding, cine-bright blood sequences, a stack of contiguous left ventricular short-axis slices (5-10 mm thick) are made from basal to apical (figure 1a) (Marcu et al. 2006). CMR is a tomographic technique that uses volumetric

quantification based on Simpson's rule. Each separate slice is distributed approximately in 30 phases (simplified in figure 1b; from 1 separate slice, 8 phases from end-diastolic to end-systolic are shown); the endocardium is traced manually in the end-diastolic and end-systolic phase. Left ventricular end-diastolic and end-systolic volume is then calculated by summation of the endocardial surfaces and multiplication by the slice thickness of each separate slice.

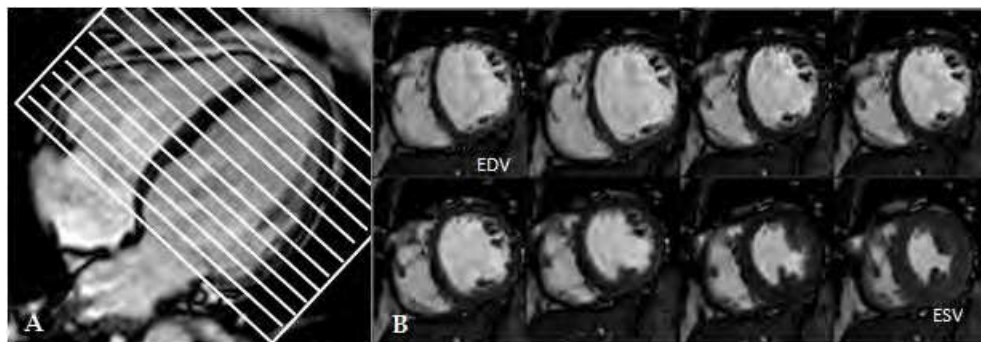


Fig. 1. Schematic figure for A: multiple short axis slices from basal to apical are made from a four chamber view, B: from 1 separate short axis slice, phases from end-diastolic to end-systolic are illustrated.

Left ventricular ejection fraction is calculated by the formula: $((\text{end-diastolic volume} - \text{end-systolic volume}) / \text{end-diastolic volume}) \times 100\%$.

Left ventricular mass can be calculated by 1. tracing the epicardium in the end-diastolic phase in each separate slice; 2. obtaining a myocardial volume by summation of the surfaces between the epicardial and endocardial lines and multiplication by the slice thicknesses; and 3. multiplication of the myocardial volume with weight density (1.05 g/cm^3) of muscle.

2.2 CE-CMR imaging for assessment of damaged myocardium

The technique of CE-CMR imaging involves an intravenous injection of a contrast agent (e.g., gadolinium at a preferred dose of 0.2 mmol/kg body weight) followed by an ECG-gated T1-weight pulse sequence 10-15 minutes after injection (5 minutes after injection if microvascular obstruction is assessed). (Jackson et al. 2007) The timing of the image acquisition is of paramount importance, as too early image acquisition reduces the difference in contrast between normal and damaged myocardium (such as scar or fibrosis) because of an insufficient washout of contrast medium from the normal myocardium; too late image acquisition, on the other hand, may result in an excessive washout from damaged myocardial tissue that leads to an inferior signal-to-noise ratio. (Vogel-Claussen et al. 2006) The typical pulse sequence for CE-CMR imaging is a segmented T1-weighted inversion-recovery-prepared fast gradient-echo sequence. An inversion-recovery pulse is used to null the signal of normal myocardium in order to optimize the difference between normal and damaged myocardial areas (which still contain contrast medium) (Figure 2).

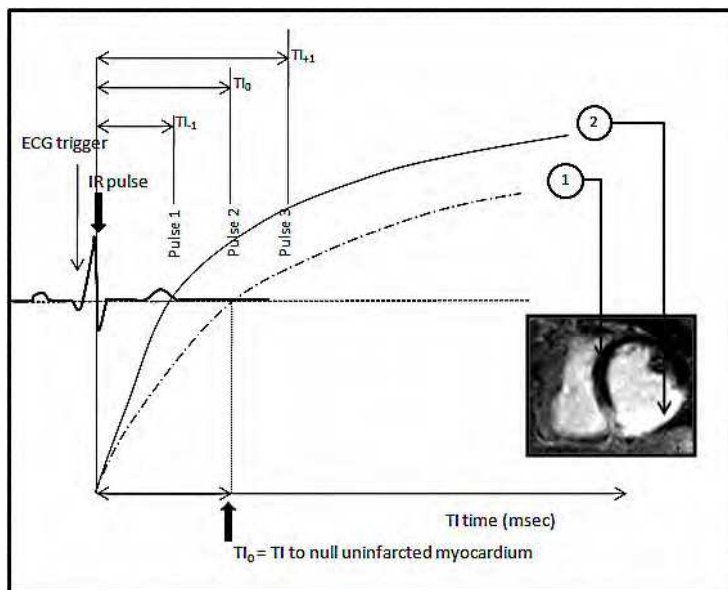


Fig. 2. Schematic figure for inversion time (TI) mapping. Following the ECG trigger, an inversion recovery (IR) pulse is applied. Before image acquisition, low-resolution TI scout images at mid-ventricular level with increasing TI (interval TI 30 msec) are performed. The optimal time to inversion (TI_0) is defined visually as the inversion time at which the uninfarcted myocardium (1) is nulled. (2) = infarcted myocardium.

The optimal inversion time depends on the contrast clearance from the normal myocardium which may show considerable inter-patient variability, depending on several factors such as the patient weight, left ventricular or renal function. Therefore, just before image acquisition, the inversion time is optimized on a per-patient basis using low-resolution scout images at mid-ventricular level with increasing inversion times at intervals of 30ms, from which the optimal inversion time can be derived (Jackson et al. 2007). The process is synchronized to the R-wave of the ECG and mid-diastolic images are acquired every other heart beat during breath-hold (Marcu et al. 2007).

2.3 T2-weighted CMR imaging for assessment of myocardial edema

T2-weighted CMR imaging is a pulse sequence sensitive to regional or global increases of myocardial water (a substantial feature of inflammatory responses) (Zagrosek et al. 2008; bdel-Aty et al. 2005). Therefore very useful in the (sub) acute phase of myocardial infarction and myocarditis. The long T2 relaxation times of water-bound protons are used to generate a water-specific contrast when applying T2-weighted sequences resulting in a high signal intensity of edematous tissue. Standard T2-weighted imaging of myocardial edema typically utilizes turbo spin-echo readouts with or without fat saturation pulses (to separate fat from water), mostly combined with dark-blood preparation (Eitel et al. 2011). An alternative acquisition mode can be the T2-prepared steady state free precession technique, which may be more reliable in imaging edema as it provides fewer artifacts and has better diagnostic accuracy than conventional darkblood acquisitions (Kellman et al. 2007).

3. CE-CMR findings in the different cardiomyopathies

3.1 CE-CMR after myocardial infarction

Myocardial infarction occurs after coronary occlusion of at least 20-30 minutes (without sufficient collateral blood supply to the affected myocardium) (Edelman, 2004). In the early phase of myocardial infarction, cellular degradation in the infarcted myocardium results in an increase in the permeability and enlargement of the extravascular space (edema), and thus, an increased distribution volume for the CMR contrast agent. Later on, due to different wash-in and wash-out kinetics, myocardial scars retain contrast agents longer than normal myocardium. The net result of both mechanisms is that infarcted myocardium appears bright on CE-T1-weighted images.

CE in patients with MI generally shows a typical pattern that is related to the perfusion area of the culprit vessel. Myocardial changes (and thus CE) of the subendocardium can generally be found which may extend to a transmural distribution in cases with prolonged coronary occlusion (Figure 3a,b).

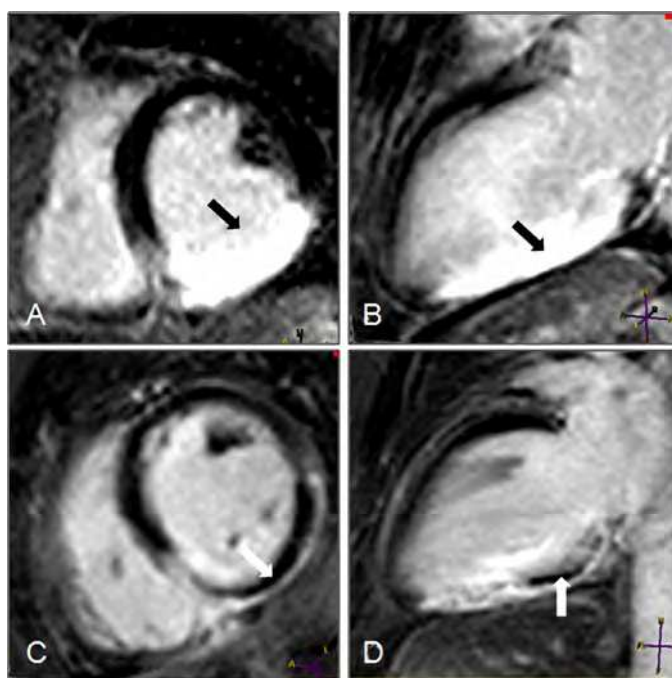


Fig. 3. CE-CMR patterns post myocardial infarction. A,B: CE short axis and long axis view showing transmural inferior infarction (black arrow). C,D: Short axis and long axis view showing an inferior infarction with microvascular obstruction (white arrow).

In patients after MI, the assessment of myocardial viability can provide clinically important information to guide further treatment because only viable myocardium may benefit from revascularization (Kim et al., 2005). Generally, a standardized 17 myocardial segment-model is used to report the results of viability assessment by CE-CMR (Figure 4) (Cerqueira et al., 2002).

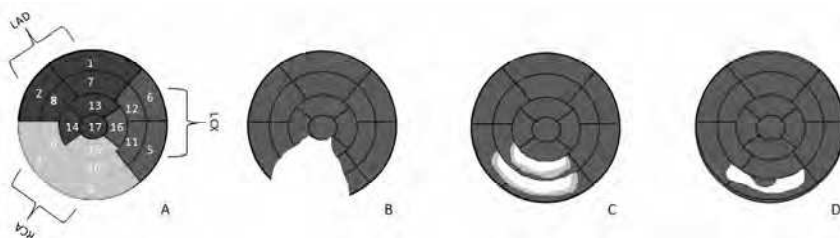


Fig. 4. Bulls eye scheme according to the 17 segmental model, demonstrating CE characteristics post myocardial infarction. A: assignment of the 17 segments to one of the 3 major coronary arteries, with segment 1, 2, 7, 8, 13, 14, and 17 corresponding to the left anterior descending coronary artery ; segments 3, 4, 9, 10 and 15 corresponding to the right coronary artery when it is dominant; and segments 5, 6, 11, 12, and 16 are assigned to the left circumflex artery. B: Transmural inferior MI. C: Inferoseptal MI with a core zone (white area) and a peri infarction zone (gray area). D: Inferior MI with microvascular obstruction (black area in myocardial infarction area).

In addition, quantification of infarcted tissue helps to prognosticate left ventricular remodeling (Orn et al., 2007). In this respect, the transmural extent of infarcted tissue as determined by CE-CMR has been shown to be a powerful predictor of the contractile response to both medical therapy and myocardial revascularization (Weinsaft et al., 2007).

Primary coronary intervention with stent implantation is meanwhile the standard for treatment of all acute ST-segment elevation myocardial infarctions, even in cases with a very challenging anatomy (Basalus et al., 2009). The early intervention rapidly restores the patency of the epicardial coronary vessels and often improves the prognosis, as is early indicated by ST-segment resolution on the electrocardiogram (van der Zwaan et al., 2010). Nowadays, aspiration of thrombi is often performed prior to stent implantation in thrombus-containing lesions in order to minimize distal embolization (Hermens et al. 2010; Stoel et al., 2009) that contributes to the development of left ventricular dysfunction after MI. In our recent CMR study, we also found that left ventricular wall motion abnormalities were significantly better in patients who underwent successful early revascularization for acute myocardial infarction (Olimulder et al., 2011).

Increasing interest is also laid on the assessment of characteristics of infarcted myocardial tissue as potential predictor of life-threatening ventricular arrhythmias. Recently, a highly significant relation between inferior MI and ventricular arrhythmias has been observed (Pascale et al. 2009). Multivariate analysis of data from 91 patients suggested that the heterogeneity of infarcted tissue (also called peri infarct zone or border zone), can be an important predictor of spontaneous ventricular arrhythmias (Roes et al., 2009).

The area of CE tends to be larger during the acute phase of MI (first week) and progressively decreases in size during the healing phase (1-4 weeks), until it reaches the state of a healed myocardial infarction (after 4 weeks) (Thygesen et al. 2007). These observations are consistent with the established pathological understanding of remodeling after MI: during the acute phase, there is myocardial edema which subsequently regresses while the necrotic myocardium is replaced by scar tissue (Marcu et al., 2007). Experimental studies have revealed that final MI size is strongly influenced by the extent of the edema in the acute phase, which is also called *area at risk*. By combining T2-weighted images to visualize myocardial edema (and thus the area at risk) and CE-CMR imaging to visualize scar (the *final infarct size*), a *myocardial salvage index* can be calculated by subtracting the infarct size from the area at risk (Aletras et al.,

2006). The myocardial salvage index has recently shown to be independently associated with adverse left ventricular remodeling and early ST-segment resolution, and may represent an interesting parameter for the assessment of novel reperfusion strategies in patients with myocardial infarction (trial registration number: NL19151.044.07).

In addition, some patients develop microvascular obstruction within the ischemic myocardial region in the acute phase of a myocardial infarction (Masci et al. 2010). Microvascular obstruction is represented by a dark zone within the infarcted region, usually located in the subendocardium because the contrast medium does not reach this area (Figure 3c,d). Its presence is associated with greater left ventricular remodeling and inferior clinical outcome. (Nijveldt et al. 2008).

3.2 CE-CMR in nonischemic cardiomyopathies

3.2.1 Hypertrophic cardiomyopathy

Hypertrophic cardiomyopathy is a primary myocardial disease characterized by focal (mostly septal) or diffuse left ventricular wall thickening (with or without left ventricular outflow obstruction). Myofibrillar hypertrophy and disarray and myocardial fibrosis have been described histologically. Inadequate capillary density and intimal hyperplasia of intramural coronary arteries, which were also seen in such patients, may contribute to myocardial ischemia (Marcu et al., 2007). There are predilection patterns of CE in patients with hypertrophic cardiomyopathies: more than 80% of patients exhibit patchy fibrosis at the right ventricular insertion points and in the anteroseptal wall in the region of characteristic septal thickening (Figure 5ab; Figure 6a) (Moon et al., 2003; Choudhury et al., 2002).

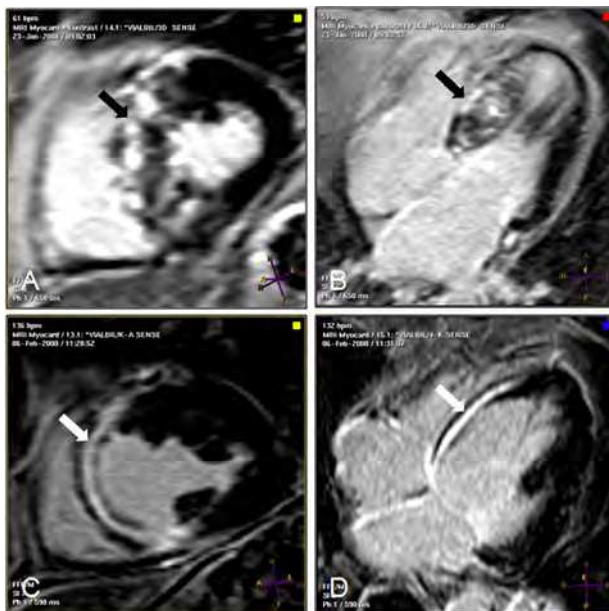


Fig. 5. CE-CMR patterns in nonischemic cardiomyopathies. A,B: CE short axis and long axis view showing hypertrophic cardiomyopathy with patchy CE septal and in the right ventricular insertion points. (black arrow). C,D: Short axis and long axis view showing dilated cardiomyopathy with CE having septal midwall predominance (white arrow).

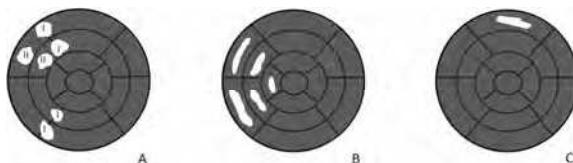


Fig. 6. Bulls eye scheme according to the 17 segmental model, demonstrating typical CE patterns in nonischemic cardiomyopathies. A: Hypertrophic cardiomyopathy with predilection CE (i.e., fibrosis) pattern at the right ventricular insertion points (I) and anteroseptal (II). Myocardial fibrosis is also located in non-hypertrophic segments. B: Idiopathic dilated cardiomyopathy with CE predominantly located in the midwall with septal predominance. C: Arrhythmogenic right ventricular cardiomyopathy with midwall CE found in the basal anterior region. CE is also found in the right ventricular outflow tract.

Myocardial fibrosis, however, is also located in non-hypertrophic segments (Bohl et al., 2008). As the amount of CE in hypertrophic cardiomyopathies often corresponds with functional parameters and the frequency of cardiac events, CE-CMR may potentially be useful for risk stratification and selection for implantable cardioverter defibrillator implantation (Rubinstein et al., 2010). Presence and extent of CE following percutaneous alcohol septal ablation for the treatment of significant left ventricular outflow tract obstruction indicates the location and extent of therapeutic myocardial tissue destruction. (Sievers et al., 2002).

3.2.2 Idiopathic dilated cardiomyopathy

Idiopathic dilated cardiomyopathy is characterized by dilation and impaired contractility of the left ventricle or both ventricles in the absence of abnormal loading conditions (e.g., arterial hypertension; valvular disease), and/or a cardiomyopathy with a distinct cause (e.g., ischemic heart disease; peripartum cardiomyopathy; toxin, chemotherapy or tachycardia induced cardiomyopathy; certain endocrinopathies) (Mueller & Attili, 2008). Histology is nonspecific and a variety of myocardial tissue alterations may occur or coexist, including myocyte hypertrophy and segmental or diffuse interstitial fibrosis. Current CE-CMR techniques are unlikely to detect diffuse fibrosis due to limited voxel resolution (Vohringer et al., 2006). Myocardial fibrosis in idiopathic dilated cardiomyopathy is mostly seen in the left ventricular midwall with septal predominance and a linear pattern (Figure 5c,d; Figure 6b); however, it has occasionally been described at subendocardial and subepicardial locations with a more patchy pattern. (Bohl et al., 2008). Of note, in various studies the prevalence of myocardial fibrosis varied from 13% to 62% (Yokokawa et al., 2009; Isbell et al., 2006). It has been suggested that the degree of CE may correlate with functional impairment of the left ventricle (Koito et al., 1996). There are preliminary data demonstrating that the presence of CE is associated with an unfavorable clinical outcome and may be a predictor of sudden death in patients with idiopathic dilated cardiomyopathy (Yokokawa et al., 2009, 2009; Assomull et al., 2009).

3.2.3 Arrhythmogenic right ventricular cardiomyopathy

The arrhythmogenic right ventricular cardiomyopathy is characterized by structural and functional abnormalities, with progressive fibrous and fatty infiltration involving variable regions of the right and left ventricular myocardium. This process finally leads to

progressive right ventricular failure and ventricular tachyarrhythmia (Bohl et al., 2008). Diagnosis of this condition remains a challenge, with nonspecific abnormalities on echocardiographic and angiographic examinations. Endomyocardial biopsy has a low sensitivity, as samples are usually taken from the septum, a region that is infrequently involved (Bohl et al., 2008). Further, endomyocardial biopsy is potential a dangerous procedure.

Information from CE-CMR may help to guide targeted endomyocardial biopsies. Predilection patterns with midwall CE are found in the basal anterior region (Figure 6c) and/or the right ventricular outflow tract. These patterns of fibrosis correlate with fibrofatty replacement of the myocardium at histologic assessment and predict induction of ventricular tachycardia during electrophysiological studies. As the presence of arrhythmogenic right ventricular cardiomyopathy cannot be ruled out based on CMR findings alone, standardized guidelines have been proposed which define major and minor criteria, including morphological, histological, electrocardiographic, functional, and genetic characteristics (McKenna et al., 1994).

3.3 CE-CMR in myocarditis

3.3.1 Myocarditis

Myocarditis is an acute or chronic inflammatory disease of the myocardium, which can be caused by viruses or initiated by post-infectious immune or primarily organ-specific autoimmune responses. (Caforio et al., 2002). Patients generally recover or infrequently develop dilated cardiomyopathy, sometimes even with life-threatening complications including severe heart failure and malignant arrhythmias (Zagrosek et al., 2008). Diagnosis of myocarditis is challenging because of a diverse clinical presentation and a limited sensitivity of endomyocardial biopsies, but may be facilitated by use of CE-CMR or myocardial global relative enhancement CMR (bdel-Aty et al., 2005; Gutberlet et al., 2008). Diagnosis of acute myocarditis is more important nowadays because of the therapeutic medical options in selected patients. (Corsten et al., 2010). Presence of CE has been reported in 44-95% of patients with myocarditis, (Mahrholdt et al., 2004, 2006) indicating areas of myocardial damage with a sensitivity of 100% and a specificity of 90% (compared to histopathology) (Mahrholdt et al., 2004). In acute myocarditis, CE is frequently located in the lateral wall, originating from the epicardium. The subendocardium is generally not involved, with the exception of eosinophilic myocarditis, which frequently involves the endomyocardium (Figure 7a). (Bohl et al., 2008; Deb et al., 2008).

In chronic myocarditis, besides an increased edema on T2-weighted imaging, an increased global relative enhancement is a common finding as confirmed in immunohistological analyses. (Gutberlet et al., 2008). CE-CMR identified areas of myocardial damage in 70% of patients with biopsy-proven chronic myocarditis and showed a predilection pattern (left ventricular midwall and/or subepicardial). In myocarditis, CE may provide additional information that could help to differentiate between viral origins, as in the majority of parvovirus B19 patients, CE is found in the lateral free wall, while in patients with human herpes virus 6 myocarditis CE frequently involves the interventricular septal midwall (Yelgec et al;2007). In addition, we recently studied a limited number of patients with chronic fatigue syndrome and concomitant ebstein barr virus or cytomegalovirus myocarditis who showed in the presence of CE a certain predilection of the septal region. Inflammatory activity on T2-weighted imaging and myocardial fibrosis on CE-CMR may

have relevant prognostic implications in acute and chronic myocarditis and may ultimately serve as a tool to triage patients. In addition, cardiac function and regression of myocardial changes can be well observed with CMR.

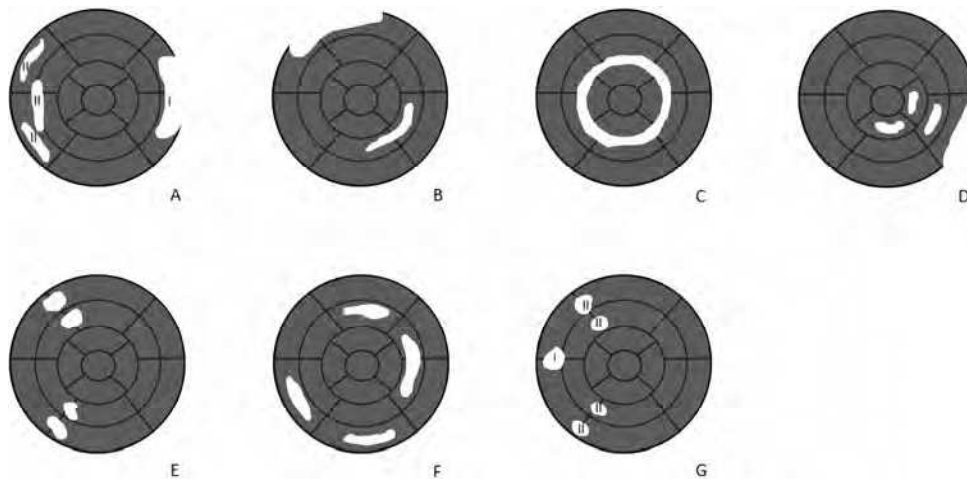


Fig. 7. Bulls eye scheme according to the 17 segmental model, demonstrating typical CE patterns in myocarditis and cardiac involvement of other diseases.

A: Myocarditis with CE frequently located in the lateral wall originating from the epicardium (I). CE patterns in myocarditis differ according to viral origin, with parvovirus B19 having CE in the lateral free wall (I), HHV6 having CE frequently in the interventricular septal midwall (II), and chronic fatigue syndrome myocarditis having CE anteroseptal and inferoseptal (III). B: Sarcoidosis with CE midwall or epicardial; however subendocardial or transmural CE may be observed. C: Amyloidosis, usually with a global diffuse CE pattern, frequently involving the subendocardium. D: Chagas' disease with CE epicardial or midwall, with a predilection pattern inferolateral. E: Pulmonary hypertension with CE involving the right ventricular insertion points and the interventricular septum. F: Muscular dystrophy with CE observed in the midwall. G: Chloroquine induced cardiomyopathy with hypertrophy and accompanying CE in the basal septum (I) and the right ventricular insertion points (I).

3.4 CE-CMR in systemic diseases inducing cardiomyopathy

3.4.1 Sarcoidosis

Cardiac involvement in sarcoidosis, a multisystem granulomatous disorder of unknown etiology, is clinically often asymptomatic (95%) while autopsy revealed cardiac manifestation in up to 60% (Patel et al., 2009). *Advanced* sarcoidosis leads to septal thinning, systolic and diastolic dysfunction, and pericardial effusion which can be detected with echocardiography (Jackson et al., 2007). *Early* sarcoidosis, however, is more challenging to diagnose, and CMR can be very useful in this context. During the acute stage of this disease, regions of active inflammation and edema are visible on T2-weighted images as areas of increased signal intensity. During the chronic stage, CE will typically appear as a midwall or epicardial nonischemic pattern (Figure 7b; figure 8).

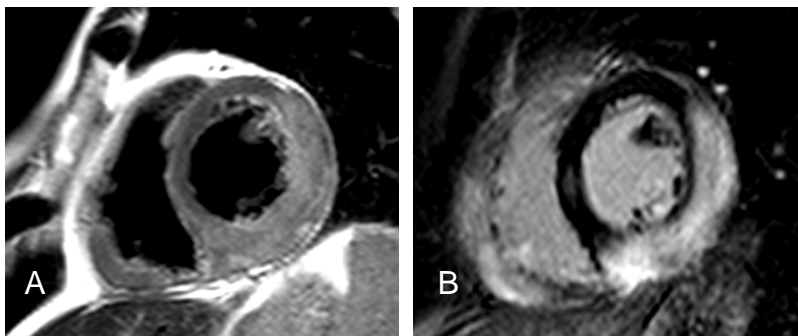


Fig. 8. CMR in a patient with sarcoidosis. A: T2 weighted imaging short axis view showing Figure 8 hyperenhancement epicardial inferior, inferolateral and anterolateral. B: Short axis view showing CE epicardial inferior, inferolateral and anterolateral.

But occasionally subendocardial or transmural CE may be observed, mimicking a pattern of post-MI. CE has been found in 50% of all patients diagnosed with sarcoidosis (Shimada et al., 2001). CE-CMR may also be useful to evaluate the response to therapy. In a CMR study of patients with sarcoidosis, CE was markedly diminished 1 month after the initiation of steroid therapy (Shimada et al., 2001). CE in sarcoidosis patients may be associated with future adverse events (including cardiac death) but confirmation in larger patient cohorts is required (Patel et al., 2009).

3.4.2 Amyloidosis

Both primary and secondary amyloidosis are characterized by extracellular deposition of fibrillar proteins (Mueller et al., 2008), which may lead to restrictive cardiomyopathy with an initially preserved systolic left ventricular function (Wynne et al., 2005). In cardiac amyloidosis, CE is commonly found as a result of the expansion of interstitial space and some endomyocardial fibrosis (Maceira et al., 2008), leading to a usually global and diffuse CE pattern (Jackson et al., 2007). Although the subendocardium is commonly involved (as in ischemic heart disease), the distribution of CE is not related to a particular coronary perfusion area (Figure 7c; figure 9) (Jackson et al., 2007).

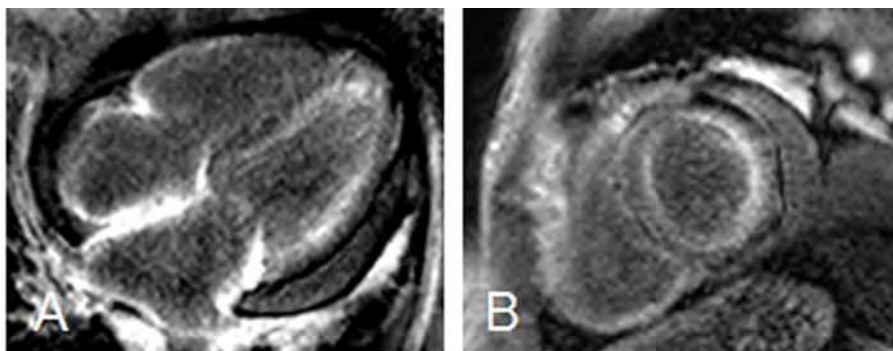


Fig. 9. CMR in a patient with amyloidosis. A,B: four chamber and short axis view showing diffuse subendocardial CE.

3.4.3 Chagas' disease

The parasitic protozoan *Trypanosoma cruzi* causes Chagas' disease, which is endemic in the Latin American region (Jackson et al., 2007). During chronic disease, the heart is the most frequently affected organ, and patients present with refractory heart failure, disorders of the conduction system, or ventricular tachycardia (Marcu et al., 2007; Rochitte et al., 2005). The fundamental pathological processes include an inflammatory response, cellular damage with a broad variation of intensity (minimal alterations up to extensive necrosis), and fibrosis (Rochitte et al., 2007). Early cardiac involvement may be detected by CE-CMR before the onset of symptoms (Rochitte et al., 2003). CE is often located epicardial or in the left ventricle midwall with a inferolateral predilection pattern (Figure 7d), but other regions - including the apex - may also sometimes be affected (Jackson et al., 2007).

3.4.4 Pulmonary hypertension

Pulmonary arterial hypertension, both primary and secondary, is characterized by an increased pulmonary vascular resistance that results in pressure overload on the right ventricle (Kovacs et al., 2008). Cine CMR permits accurate assessment of right ventricular mass and volumes which is often difficult to accomplish with other imaging modalities (Marcu et al., 2007). Myocardial CE is frequently observed in patients with severe symptomatic pulmonary artery hypertension with predilection patterns involving both right ventricular septal insertion points and the interventricular septum (Figure 7e). CE in the interventricular septum was found to be associated with septal bowing (on cine CMR), and the extent of CE correlated inversely with right ventricular systolic function (Blyth et al., 2005).

3.4.5 Muscular dystrophy

Both Becker and Duchenne muscular dystrophies are progressive X chromosome-linked recessive neuromuscular diseases with myocardial involvement in up to 72% of patients showing a mildly reduced left ventricular function up to severe left ventricular impairment and dilated cardiomyopathy. Cardiac myocyte dystrophin deficiency leads to necrosis causing replacement of damaged myocardium by connective tissue and fat in both ventricles. On CE-CMR, hyperenhancement is predominantly seen in left ventricular midwall (Figure 7f) and has been described in 73-100% of patients (Yilmaz et al., 2008). Early diagnosis of myocardial involvement as assessed with CE-CMR may permit an earlier treatment of heart failure which could increase life expectancy.

3.4.6 Chloroquine-induced cardiomyopathy

Chloroquine-induced cardiomyopathy is a rare iatrogenic disease that is associated with long-term intake of chloroquine, which is most frequently prescribed for treatment of rheumatoid arthritis and malaria prophylaxis (Reffelman et al., 2006). This cardiomyopathy is characterized by ineffective lysosomal metabolism because of an increase in pH that leads to accumulation of lysosomal glycosphingolipids and finally thickening of cardiac walls (Pieroni et al., 2007). The time interval between the start of chloroquine therapy and disease manifestation varies greatly, ranging from several months to more than 20 years (Reffelman et al., 2006). CMR may demonstrate the presence of left ventricular hypertrophy with accompanying areas of CE in the basal septum and at the insertion point of the right ventricle (Figure 7g).

Fabry disease, an X chromosome-linked lysosomal storage disease caused by a deficient activity of the enzyme α -galactosidase A, can also result in the accumulation of glycosphingolipids in multiple organs, including the heart (Pieroni et al., 2007; Gange et al., 2009). Fabry disease cardiomyopathy should therefore always be considered in the differential diagnosis of “idiopathic” left ventricular hypertrophy (in the absence of arterial hypertension or valvular disease).

3.5 CE-CMR in other diseases inducing cardiomyopathy

3.5.1 Tsako Tsubo cardiomyopathy

This relatively ‘novel’ cardiomyopathy is characterized by acute but rapidly reversible distinctive regional left ventricular dysfunction, in the absence of significant coronary artery disease. Japanese investigators were intrigued by the unusual end-systolic shape of the left ventricle, resembling the original Japanese octopus trap (figure 10a) (Sharkey et al., 2011).



Fig. 10. CMR of a patient with tsako tsubo. A: cine four chamber view with characteristic end-systolic apical ballooning. B,C: four chamber and short axis view with no presence of CE in the myocardium.

Consequently, the term tsako tsubo cardiomyopathy was introduced in 1990. Several pathophysiological mechanisms have been proposed, including multivessel coronary spasm, catecholamine induced myocardial stunning, coronary emboli with spontaneous fibrinolysis, and myocardial inflammation (Eitel et al., 2010). Recently, variant forms are described, including inverted tako-tsubo and mid-ventricular ballooning cardiomyopathy (Marti et al., 2009; Yasu et al., 2006).

In the setting of tako tsubo cardiomyopathy, CMR may identify increased myocardial mass and myocardial edema (using T2-weighted imaging) as well as the normalization of these parameters as the left ventricular dysfunction improves. (Stensaeth et al. 2011). Of important note, (with only a few exceptions, reported in literature) (Koeth et al. 2008) no CE is present in this disease, consistent with preserved myocardial viability, as reflected by the transient nature of left ventricular dysfunction (figure10b) (Eitel et al, 2010; Deetjen et al., 2006) .At follow up, there is complete normalization of left ventricular function, in the absence of CE, edema and pericardial effusion (Eitel et al., 2010; Koeth et al., 2008). The lack of CE (initial and follow up) allows thus for distinction between different causative aetiologies including MI, infiltrative diseases and cases of myocarditis.

Therefore, CMR in combination with T2 weighted imaging and CE may provide valuable additional information for the differential diagnoses and therapeutic decision-making in patients with suspected tako tsubo cardiomyopathy.

3.5.2 Noncompaction cardiomyopathy

Left ventricular noncompaction cardiomyopathy is characterized by a thin, compacted epicardial layer and a thick endocardial layer with prominent trabeculation and deep recesses (figure 11) (Jacquier et al.).

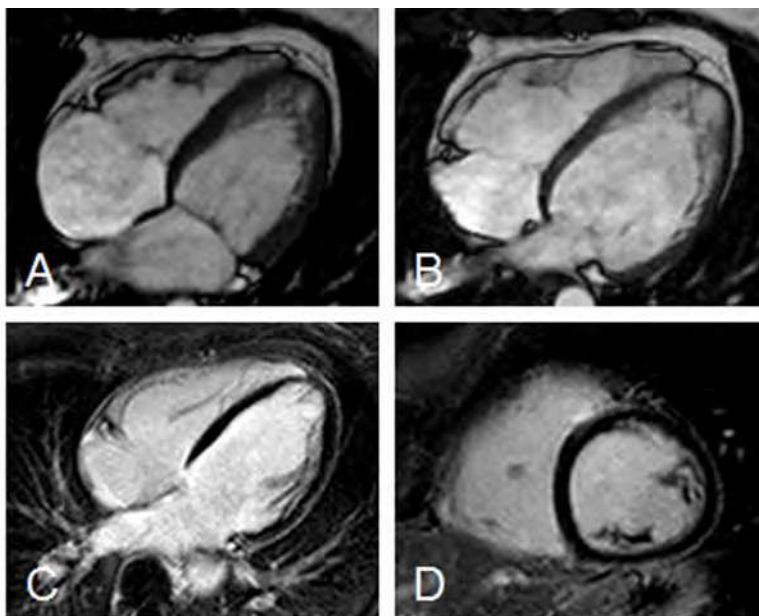


Fig. 11. Patient with noncompaction cardiomyopathy. A,B: end-systolic and end-diastolic four chamber view with characteristic prominent trabeculation and deep recesses. C,D: four chamber and short axis view with no presence of CE.

It can occur isolated or in association with numerous congenital cardiac malformations, including atrial and ventricular septal defects, aortic stenosis, and aortic calcification. It is usually diagnosed in pediatric age. Accurate diagnostic criteria are clinically important as it is associated with severe left ventricular dysfunction, thrombo-embolism, and ventricular arrhythmia. According to Jacquier et al., a CMR-assessed trabeculated left ventricular mass above 20% of the global left ventricular mass is highly sensitive and specific for the diagnosis of left ventricular noncompaction. Right ventricular noncompaction which can be easily assessed with CMR, is reported in up to 60% of patients (Dursun et al., 2010). Recently, Dursun et al. found that presence of CE (fibrosis) was found in 70% of the investigated patients with left ventricular noncompaction. Dodd et al, showed that the amount of CE in patients with left ventricular noncompaction is inversely related with left ventricular ejection fraction (Dodd et al., 2007). The presence of CE is thus probably of bad prognosis in this disease (Jacquier et al., 2010).

3.5.3 CE-CMR imaging in chemotherapy induced cardiomyopathy

Several chemotherapeutic therapies in the setting of malignant diseases have been associated with the development of cardiac failure. Chemotherapies with a high incidence of cardiac failure are anthracyclines (doxorubicin) 3-26%, and monoclonal antibodies (trastuzumab) 2-28% (Yeh et al., 2009). The cumulative dose (especially doxorubicin; cumulative dose 550 mg/m²), the administration schedule, concomitant use of other cardiotoxic therapies, and a history of cardiovascular disease, determines the likelihood of inducing cardiomyopathy.

Little is known about the utility of CE-CMR in the assessment of chemotherapy induced cardiomyopathy. Fallah-Rad et al. reported in 10 out of 160 breast cancer patients with trastuzumab induced cardiomyopathy (left ventricular ejection fraction < 40%), presence of epicardial CE. Recently, Kirthy et al. studied (using CE-CMR) 12 breast cancer patients with adjuvant trastuzumab; whereas left ventricular dysfunction was observed, no evidence of necrosis or fibrosis was found in any of the patients (Kirthy et al., 2011). Data on other chemotherapy induced cardiomyopathy assessed with CE-CMR are scarce (Lightfoot et al., 2010; Wassmuth et al., 2001; Wu et al., 2009). Therefore, further studies are needed to validate the usefulness of CE-CMR as a marker for (irreversible) left ventricular dysfunction and development as well as prevention of cardiac failure when chemotherapy is given.

4. Guided endomyocardial biopsy

CE patterns on CMR imaging may also help to guide endomyocardial biopsies as scar/fibrosis patterns on CE-CMR may serve as a map for the exact location to accomplish endomyocardial biopsies if necessary; thus enhancing the diagnostic accuracy. A small study has indeed confirmed that the diagnostic performance of endomyocardial biopsies is increased when biopsies are obtained from the region of CE in the case of myocarditis (Mahrholdt et al., 2004, 2006). However, according to Yilmaz et al. who were unable to confirm the value of CE-CMR for guiding endomyocardial biopsies, endomyocardial biopsies exactly obtained from the region of CE may sometimes be impracticable as the area of CE may be small and as a consequence cannot exactly be reached by the biotome because of the limited steerability of the biotome (Yilmaz et al., 2010).

5. Screening for cardiomyopathy

Cardiomyopathy can occur as part of inherited syndromes. In the case of hypertrophic cardiomyopathy, over 900 gene mutations have been linked. The gene mutations predominantly encode for contractile proteins, such as cardiac myosin-binding protein C (MYBPC3) and beta-myosin heavy chain (MYH7) (thick filament of the sarcomere), and troponin T and troponin I (encoding for thin filament of the sarcomere; accounting for ≈ 6% of the hypertrophic cardiomyopathy-causing mutations). Next to sarcomeric mutations, several metabolic disorders are linked to the hypertrophic cardiomyopathy phenotype, such as Fabry disease (as mentioned above), an X chromosome-linked lysosomal storage disease (Brouwer et al., 2011). Thus, there is currently no consensus of a definitive screening test based on genetic studies for hypertrophic cardiomyopathy. Additionally, genetic screening can not differentiate between gene carriers who express the disease and those who do not (Devlin et al., 2000). As a consequence, the heterogeneous expression includes patients suffering from severe symptomatic hypertrophic cardiomyopathy (diminished left ventricular function and fibrosis of the myocardium) as well as asymptomatic individuals.

CE-CMR imaging is able to provide accurate assessment of functional parameters and myocardial disorders in one single examination. Therefore, familial screening (especially in autosomal dominant disorders) with CE-CMR may be of utmost importance as individual findings may have significant therapeutic consequences.

As an example, in our tertiary centre, an 18 year old female patient was diagnosed with familiar hypertrophic cardiomyopathy (cardiac myosin-binding protein C). CE-CMR imaging revealed assymetrical septal hypertrophy (septal thickness 38 mm) and presence of fibrosis (figure 12).

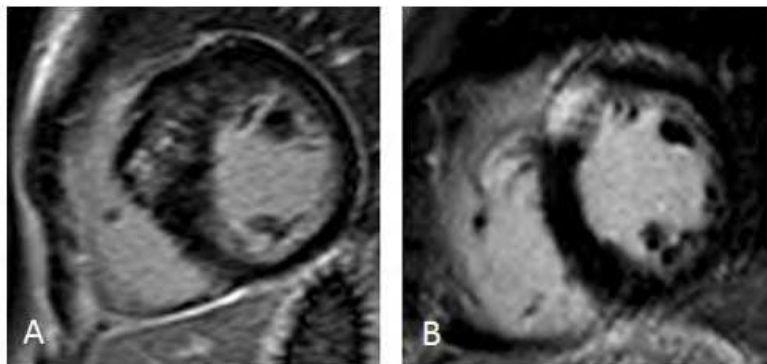


Fig. 12. Screening a relative for cardiomyopathy A. 18 year old female patient with genetic disorder cardiac myosin-binding protein C. Short axis view showing assymetrical septal hypertrophy with CE anteroseptal. B. 56 year old male patient (father) with the same genetic disorder. Short axis view showing identical CE anteroseptal.

Following the guidelines (septal thickness >30 mm) in addition with a medical history of a collapse, she was selected for implantable cardioverter defibrillator therapy (Maron et al., 2003). Her father, (familiar screened and having the same genetic disorder) showed the same pattern of assymetrical septal hypertrophy (septal thickness 24 mm) and presence of fibrosis with CE-CMR imaging, following the guidelines not an indication for implantable cardioverter defibrillator therapy. As mentioned earlier, the amount of CE in hypertrophic cardiomyopathies often corresponds with functional parameters and the frequency of cardiac events, therefore CE-CMR may potentially be useful for risk stratification and selection for implantable cardioverter defibrillator implantation.

6. Future developments

Several new strategies for the treatment of the various forms of cardiomyopathy are currently subject of research, including the transplantation of primitive cell types (e.g., stem cells or myoblasts) into damaged myocardium in an attempt to promote trans-differentiation into functional myocardial cells. CE-CMR imaging can be used to monitor such studies and to evaluate the results of novel therapeutic strategies such as direct injection of primitive cell types into segments with transmural infarction. (Orlic et al., 2002). In animal models, mesenchymal stem cells have been labeled with iron-based contrast agents to examine the process of “homing” of such cells in the myocardium (Hill et al., 2003; Kraitichman et al., 2003; Garot et al., 2003).

Recently, 3.0 T CMR imaging with a 3D inversion-recovery gradient-echo sequence was compared to standard 2D imaging. The 3D technique showed superior spatial image resolution, shorter image acquisition time, preserved contrast-to-noise ratio, and similar intra and interobserver variabilities (compared to the 2D approach), which could improve the clinical utility of CE-CMR in the future (Bauner et al., 2009). At higher heart rates, though, motion artifacts can be seen.

7. Conclusion

CE-CMR is increasingly used to establish the etiology, monitor therapeutic strategies (follow up), and obtain prognostic information in a variety of cardiomyopathies. While CE-CMR can provide valuable information, there is considerable overlap in CE patterns. For that reason, CE-CMR findings should always be considered in the light of the clinical history and presentation as well as findings obtained from other diagnostic modalities. Development in CMR hardware and software are required for the ability to perform tissue characterization which fully corresponds with histopathological findings.

8. References

- Aletras, AH.; Tilak, GS.; Natanzon, A.; Hsu, LY.; Gonzalez, FM.; Hoyt, RF. & Arai AE. (2006). Retrospective determination of the area at risk for reperfused acute myocardial infarction with T2-weighted cardiac magnetic resonance imaging: histopathological and displacement encoding with stimulated echoes (DENSE) functional validations. *Circulation*, Vol.113, No.15, (April 2006), pp. 1865-1870.
- Amado, LC.; Gerber, BL.; Gupta, SN.; Rettman, DW.; Szarf, G.; Schock, B.; Nasir K.; Kraitchman, DL.; & Lima, JA. (2004). Accurate and objective infarct sizing by contrast-enhanced magnetic resonance imaging in a canine myocardial infarction model. *J Am Coll Cardiol*, Vol.44, No.12, (December 2004), pp.2383-2389.
- Assomull, RG.; Prasad, SK.; Lyne, J.; Smith, G.; Burman, ED.; Khan, M.; Sheppard MN.; Poole-Wilson, PA. & Pennell DJ. (2006). Cardiovascular magnetic resonance, fibrosis, and prognosis in dilated cardiomyopathy. *J Am Coll Cardiol*, Vol.48, No10, (November 2006), pp. 1977-1985.
- Basalus, M.; Louwerenburg, JW.; van Houwelingen, KG.; Stoel, MG. & von Birgelen, C. (2009). Primary percutaneous coronary intervention in the left main stem of a monocoronary artery. *Neth Heart J*, Vol.17 No.7-8, (Augustus 2009), pp. 274-276.
- Bauner, KU.; Muehling, O.; Theisen, D.; Hayes, C.; Wintersperger, BJ.; Reiser, MF. & Huber, AM. (2009). Assessment of Myocardial Viability with 3D MRI at 3 T. *AJR Am J Roentgenol*, Vol.192, No.6, (Juny 2009), pp. 1645-1650.
- bdel-Aty, H.; Boye, P.; Zagrosek, A.; Wassmuth, R.; Kumar, A.; Messroghli, D.; Bock, P.;
- Dietz, R.; Friedrich, MG. & Schulz-Menger J. (2005). Diagnostic performance of cardiovascular magnetic resonance in patients with suspected acute myocarditis: comparison of different approaches. *J Am Coll Cardiol*, Vol.45, No11, (Juny 2005), pp. 1815-1822.
- Bello, D.; Fieno, DS.; Kim, RJ.; Pereles, FS.; Passman, R.; Song, G.; Kadish, AH. & Goldberger, JJ. (2005). Infarct morphology identifies patients with substrate for sustained ventricular tachycardia. *J Am Coll Cardiol*, Vol.45, No7, (April 2005), pp. 1104-1108.

- Blyth, KG.; Groenning, BA.; Martin, TN.; Foster, JE.; Mark, PB.; Dargie, HJ. & Peacock, AJ. (2005). Contrast enhanced-cardiovascular magnetic resonance imaging in patients with pulmonary hypertension. *Eur Heart J*, Vol.26, No.19, (Oktober 2005), pp. 1993-1999.
- Bohl, S.; Wassmuth, R.; bdel-Aty, H.; Rudolph, A.; Messroghli, D.; Dietz, R. & Schulz-Menger, J. (2008). Delayed enhancement cardiac magnetic resonance imaging reveals typical patterns of myocardial injury in patients with various forms of non-ischemic heart disease. *Int J Cardiovasc Imaging*, Vol.24, No.6, (Augustus 2008), pp. 597-607.
- Brouwer, WP.; van Dijk, SJ.; Stienen, GJ.; van Rossum, AC.; van der Velden, J. & Germans T. (2011). The development of familial hypertrophic cardiomyopathy: from mutation to bedside. *Eur J Clin Invest*, Vol.41, No.5, (May 2011), pp. 568-578.
- Caforio, AL.; Mahon, NJ.; Tona, F. & McKenna, WJ. (2002). Circulating cardiac autoantibodies in dilated cardiomyopathy and myocarditis: pathogenetic and clinical significance. *Eur J Heart Fail*, Vol.4, No.4 (Augustus 2002), pp. 411-417.
- Cerqueira, MD.; Weissman, NJ.; Dilsizian, V.; Jacobs, AK.; Kaul, S.; Laskey, WK.; Pennell, DJ.; Rumberger, JA.; Ryan, T. & Verani MS. (2002). Standardized myocardial segmentation and nomenclature for tomographic imaging of the heart: a statement for healthcare professionals from the Cardiac Imaging Committee of the Council on Clinical Cardiology of the American Heart Association. *Circulation*, Vol.105, No.4, (January 2002), pp. 539-542.
- Choudhury, L.; Mahrholdt, H.; Wagner, A.; Choi, KM.; Elliott, MD.; Klocke, FJ.; Bonow, RO.; Judd, RM. & Kim, RJ. (2002). Myocardial scarring in asymptomatic or mildly symptomatic patients with hypertrophic cardiomyopathy. *J Am Coll Cardiol*, Vol.40, No.12 (December 2002), pp. 2156-2164.
- Corsten, MF.; Dennert, R.; Jochems, S.; Kuznetsova, T.; Devaux, Y.; Hofstra, L.; Wagner, DR.; Staessen, JA.; Heymans, S. & Schroen B. (2010). Circulating MicroRNA-208b and MicroRNA-499 reflect myocardial damage in cardiovascular disease. *Circ Cardiovasc Genet*, Vol.3, No.6 (December 2010), pp. 499-506.
- Deb, K.; Djavidani, B.; Buchner, S.; Poschenrieder, F.; Heinicke, N.; Feuerbach, S.; Riegger, G. & Luchner A. (2008). Time course of eosinophilic myocarditis visualized by CMR. *J Cardiovasc Magn Reson*, Vol.10, No.1, (2008), pp. 21.
- Deetjen, AG.; Conradi, G.; Mollmann, S.; Rad, A.; Hamm, CW. & Dill T. (2006). Value of gadolinium-enhanced magnetic resonance imaging in patients with Tako-Tsubo-like left ventricular dysfunction. *J Cardiovasc Magn Reson*, Vol.8, No.2, (2006), pp. 367-372.
- Devlin, AM. & Ostman-Smith, I. (2000). Diagnosis of hypertrophic cardiomyopathy and screening for the phenotype suggestive of gene carriage in familial disease: a simple echocardiographic procedure. *J Med Screen* 2000, Vol.7, No.2, (2000), pp. 82-90.
- Dodd, JD.; Holmvang, G.; Hoffmann Ferencik, M.; Abbara, S.; Brady, TJ. & Cury RC. (2007). Quantification of left ventricular noncompaction and trabecular delayed hyperenhancement with cardiac MRI: correlation with clinical severity. *AJR Am J Roentgenol*, Vol.189, No.4, (Oktober 2007), pp. 974-980.
- Dursun, M.; Agayev, A.; Nisli, K.; Ertugrul, T.; Onur, I.; Oflaz, H. & Yekeler E. (2010). MR imaging features of ventricular noncompaction: emphasis on distribution and pattern of fibrosis. *Eur J Radiol* 2010, Vol.74, No.1, (April 2010), pp. 147-151.
- Edelman, RR. (2004) Contrast-enhanced MR imaging of the heart: overview of the literature. *Radiology*, Vol.232, No.3, (September 2004), pp. 653-668.

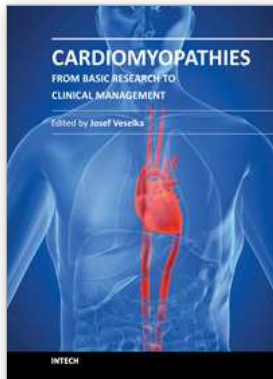
- Eitel, I.; Lucke, C.; Grothoff, M.; Sareban, M.; Schuler, G.; Thiele, H. & Gutberlet M. (2010). Inflammation in takotsubo cardiomyopathy: insights from cardiovascular magnetic resonance imaging. *Eur Radiol*, Vol.20, No.2 (February 2010), pp. 422-431.
- Eitel, I. & Friedrich, MG. (2011) T2-weighted cardiovascular magnetic resonance in acute cardiac disease. *J Cardiovasc Magn Reson*, Vol.13, (2011), pp. 13.
- Gange, CA.; Link, MS. & Maron MS. (2009). Utility of cardiovascular magnetic resonance in the diagnosis of Anderson-Fabry disease. *Circulation*, Vol.120, No.13, (September 2009), pp. 96-97.
- Garot, J.; Untersee, T.; Teiger, E.; Champagne, S.; Chazaud, B.; Gherardi, R.; Hittinger, L.; Gueret, P. & Rahmouni A. (2003). Magnetic resonance imaging of targeted catheter-based implantation of myogenic precursor cells into infarcted left ventricular myocardium. *J Am Coll Cardiol*, Vol.41, No.10, (May 2003), pp. 1841-1846.
- Gutberlet, M.; Spors, B.; Thoma, T.; Bertram, H.; Denecke, T.; Felix, R.; Noutsias, M.; Schultheiss, HP. & Kuhl U. (2008). Suspected chronic myocarditis at cardiac MR: diagnostic accuracy and association with immunohistologically detected inflammation and viral persistence. *Radiology*, Vol.246, No.2, (February 2008), pp. 401-409.
- Hermens, JA.; van Houwelingen, GK.; de Man, FH.; Louwerenburg, HW. & von Birgelen C. (2010). Thrombus aspiration in a series of patients with stable or unstable angina pectoris and lesion-site thrombus formation. *Neth Heart J*, Vol. 18, No.9 (September 2010), pp. 423-429.
- Hill, JM.; Dick, AJ.; Raman, VK.; Thompson, RB.; Yu, ZX.; Hinds, KA.; Pessanha, BS.; Guttman, MA.; Varney, TR.; Martin, BJ.; Dubar, CE.; McVeigh, ER. & Lederman RJ. (2003). Serial cardiac magnetic resonance imaging of injected mesenchymal stem cells. *Circulation*, Vol.108, No.8, (August 2003), pp. 1009-1014.
- Hsu, LY.; Natanzon, A.; Kellman, P.; Hirsch, GA.; Aletras, AH. & Arai AE. (2006). Quantitative myocardial infarction on delayed enhancement MRI. Part I: Animal validation of an automated feature analysis and combined thresholding infarct sizing algorithm. *J Magn Reson Imaging*, Vol.23, No.3 (March 2006), pp. 298-308.
- Isbell, DC. & Kramer, CM. (2006). The evolving role of cardiovascular magnetic resonance imaging in nonischemic cardiomyopathy. *Semin Ultrasound CT MR*, Vol.27, No.1 (February 2006), pp. 20-31.
- Jackson, E. Bellenger, N.; Seddon, M.; Harden, S. & Peebles C. (2007). Ischaemic and non-ischaemic cardiomyopathies--cardiac MRI appearances with delayed enhancement. *Clin Radiol*, Vol.62, No.5 (May 2007), pp. 395-403.
- Jacquier, A.; Thuny, F.; Jop, B.; Giorgi, R.; Cohen, F.; Gaubert, JY.; Vidal, V.; Bartoli, JM.; Habib, G. & Moulin G. (2010). Measurement of trabeculated left ventricular mass using cardiac magnetic resonance imaging in the diagnosis of left ventricular non-compaction. *Eur Heart J*, Vol.31, No.9, (May 2010), pp. 1098-1104.
- Kellman, P.; Aletras, AH.; Mancini, C.; McVeigh, ER. & Arai, AE. (2007) T2-prepared SSFP improves diagnostic confidence in edema imaging in acute myocardial infarction compared to turbo spin echo. *Magn Reson Med*, Vol.57, No.5, (May 2007), pp.891-897.
- Kim, RJ.; Wu, E.; Rafael, A.; Chen, EL.; Parker, MA.; Simonetti, O.; Klocke, FJ.; Bonow, RO. & Judd, RM. (2000). The use of contrast-enhanced magnetic resonance imaging to identify reversible myocardial dysfunction. *N Engl J*, Vol.343, No.20, (November 2000), pp. 1445-1453.
- Kirthy, V.; Schultz, C. & Davies S. (2011). Cardiac Imaging of trastuzumab-induced cardiomyopathy. *European Journal of Heart Failure Supplements*, Vol.10, (2011) Koeth,

- O.; Mark, B.; Kilkowski, A.; Layer, G.; Cornelius, B.; Kouraki, K.; Bauer, T.; Zahn, R.;
- Senges, J. & Zeymer U. (2008). Clinical, angiographic and cardiovascular magnetic resonance findings in consecutive patients with Takotsubo cardiomyopathy. *Clin Res Cardiol*, Vol.97, No.9, (September 2008), pp. 623-627.
- Koito, H.; Suzuki, J.; Ohkubo, N.; Ishiguro, Y.; Iwasaka, T. & Inada M. (1996). Gadolinium-diethylenetriamine pentaacetic acid enhanced magnetic resonance imaging of dilated cardiomyopathy: clinical significance of abnormally high signal intensity of left ventricular myocardium. *J Cardiol*, Vol.28, No1. (July 1996), pp. 41-49.
- Kovacs, G.; Reiter, G.; Reiter, U.; Rienmuller, R.; Peacock, A. & Olschewski H. (2008). The emerging role of magnetic resonance imaging in the diagnosis and management of pulmonary hypertension. *Respiration*, Vol.76, No.4, (2008), pp. 458-470.
- Kraitchman, DL.; Heldman, AW.; Atalar, E.; Amado, LC.; Martin, BJ.; Pittenger, MF.; Hare, JM. & Bulte JW. (2003). In vivo magnetic resonance imaging of mesenchymal stem cells in myocardial infarction. *Circulation*, Vol.107, No.18, (May 2003), pp. 2290-2293.
- Lightfoot, JC.; D'Agostino, RB.; Jr., Hamilton, CA.; Jordan, J.; Torti, FM.; Kock, ND.; Jordan, J.; Workman, S. & Hundley WG. (2010). Novel approach to early detection of doxorubicin cardiotoxicity by gadolinium-enhanced cardiovascular magnetic resonance imaging in an experimental model. *Circ Cardiovasc Imaging* 2010, Vol.3, No.5, (September 2010), pp. 550-558.
- Maceira, AM.; Prasad, SK.; Hawkins, PN.; Roughton, M. & Pennell DJ. (2008). Cardiovascular magnetic resonance and prognosis in cardiac amyloidosis. *J Cardiovasc Magn Reson*, Vol.10, No.1, (2008), pp. 54.
- Mahrholdt, H.; Goedecke, C.; Wagner, A.; Meinhardt, G.; Athanasiadis, A.; Vogelsberg, H.; Fritz, P.; Klingel, K.; Kandolf, R. & Sechtem U. (2004). Cardiovascular magnetic resonance assessment of human myocarditis: a comparison to histology and molecular pathology. *Circulation*, Vol.109, No.10, (March 2004), pp. 1250-1258.
- Mahrholdt, H.; Wagner, A.; Deluigi, CC.; Kispert, E.; Hager, S.; Meinhardt, G.; Vogelsberg, H.; Fritz, P.; Dippon, J.; Bock, CT.; Klingel, K.; Kandolf, R. & Sechtem U. (2004). Presentation, patterns of myocardial damage, and clinical course of viral myocarditis. *Circulation*, Vol.114, No.15, (Oktober 2006), pp. 1581-1590.
- Marcu, CB.; Beek, AM. & van Rossum, AC. (2006). Clinical applications of cardiovascular magnetic resonance imaging. *CMAJ*, Vol.175, No.8, (Oktober 2006), pp. 911-917.
- Marcu, CB.; Nijveldt, R.; Beek, AM. & van Rossum, AC. (2007). Delayed contrast enhancement magnetic resonance imaging for the assessment of cardiac disease. *Heart Lung Circ*, Vol.16, No.2, (April 2007), pp70-78
- Maron, BJ.; McKenna, WJ.; Danielson, GK.; Kappenberger, LJ.; Kuhn, HJ.; Seidman, CE.; Shah, PM.; Spencer. WH.; Spirito, P.; Ten Cate, FJ. & Wigle ED. (2002). American College of Cardiology/European Society of Cardiology clinical expert consensus document on hypertrophic cardiomyopathy. A report of the American College of Cardiology Foundation Task Force on Clinical Expert Consensus Documents and the European Society of Cardiology Committee for Practice Guidelines. *J Am Coll Cardiol*, Vol.42, No.9, (March 2003), pp. 1687-1713
- Orlic, D.; Hill, JM. & Arai AE. (2002). Stem cells for myocardial regeneration. *Circ Res*, Vol.91, No.12, (December 2002), pp. 1092-1102.
- Marti, V.; Carreras, F.; Pujadas, S. & De Rozas JM. (2009). Transient left ventricular basal ballooning-"inverted" Tako-tsubo. *Clin Cardiol*, Vol.32. No.7, (September 2009), pp. 20-21.

- Masci, PG.; Ganame, J.; Strata, E.; Desmet, W.; Aquaro, GD.; Dymarkowski, S.; Valenti, V.; Janssens, S.; Lombardi, M.; Van de Werf.; L'Abbate, A. & Bogaert J. (2010). Myocardial salvage by CMR correlates with LV remodeling and early ST-segment resolution in acute myocardial infarction. *JACC Cardiovasc Imaging*, Vol.3, No.1, (January 2010), pp. 45-51.
- McKenna, WJ.; Thiene, G.; Nava, A.; Fontaliran, F.; Blomstrom-Lundqvist, C.; Fontaine, G. & Camerini F. (1994). Diagnosis of arrhythmogenic right ventricular dysplasia/cardiomyopathy. Task Force of the Working Group Myocardial and Pericardial Disease of the European Society of Cardiology and of the Scientific Council on Cardiomyopathies of the International Society and Federation of Cardiology. *Br Heart J*, Vol.71, No.3, (March 1994), pp. 215-218.
- Moon, JC.; McKenna, WJ.; McCrohon, JA.; Elliott, PM.; Smith, GC. & Pennell DJ. (2003). Toward clinical risk assessment in hypertrophic cardiomyopathy with gadolinium cardiovascular magnetic resonance. *J Am Coll Cardiol*, Vol.41, No.9 (May 2003), pp. 1561-1567.
- Mueller, GC. & Attili A. Cardiomyopathy: magnetic resonance imaging evaluation. *Semin Roentgenol*, Vol.43, No.3, (July 2008), pp. 204-222.
- Nijveldt, R.; Beek, AM.; Hirsch, A.; Stoel, MG.; Hofman, MB.; Umans, VA.; Algra, PR.; Twisk, JW. & van Rossum AC. (2008). Functional recovery after acute myocardial infarction: comparison between angiography, electrocardiography, and cardiovascular magnetic resonance measures of microvascular injury. *J Am Coll Cardiol*, Vol.52, No3. (July 2008), pp. 181-189.
- Olimulder, MA.; Galjee, MA.; van Es, J.; Wagenaar, LJ.; von Birgelen, C. (2011). Contrast-enhancement cardiac magnetic resonance imaging beyond the scope of viability. *Neth Heart J*, Vol.19, No.5 (May 2011), pp. 236-245.
- Olimulder, MA.; Kraaier, K.; Galjee, MA.; Scholten, MF.; van Es, J.; Wagenaar, LJ.; van der Palen, J. & von Birgelen, C. (2011). Infarct tissue characteristics of patients with versus without early revascularization for acute myocardial infarction: a contrast-enhancement cardiovascular magnetic resonance imaging study. *Heart Vessels*, (May 2011).
- Orn, S.; Manhenke, C.; Anand, IS.; Squire, I.; Nagel, E.; Edvardsen, T. & Dickstein K. (2007). Effect of left ventricular scar size, location, and transmurality on left ventricular remodeling with healed myocardial infarction. *Am J Cardiol*, Vol.99, No.8 (April 2007), pp. 1109-1114.
- Pascale, P.; Schlaepfer, J.; Oddo, M.; Schaller, MD.; Vogt, P. & Fromer M. (2009). Ventricular arrhythmia in coronary artery disease: limits of a risk stratification strategy based on the ejection fraction alone and impact of infarct localization. *Europace*, Vol.11, No.12, (December 2009), pp. 1639-1646.
- Patel, MR.; Cawley, PJ.; Heitner, JF.; Klem, I.; Parker, MA.; Jaroudi, WA.; Meine, TJ.; White', JB.; Elliott, MD.; Kim, HW.; Judd, RM. & Kim RJ. (2009). Detection of myocardial damage in patients with sarcoidosis. *Circulation*, Vol.120, No.20, (November 2009), pp. 1969-1977.
- Pieroni, M.; Bellocci, F. & Crea F. (2007). Letter by Pieroni et al regarding article, "Contrast-enhanced magnetic resonance imaging of a patient with chloroquine-induced cardiomyopathy confirmed by endomyocardial biopsy". *Circulation*, Vol.115, No.5 (February 2007), pp. 67.
- Reffelmann, T.; Naami, A.; Spuentrup, E. & Kuhl HP. (2006). Images in cardiovascular medicine. Contrast-enhanced magnetic resonance imaging of a patient with

- chloroquine-induced cardiomyopathy confirmed by endomyocardial biopsy. *Circulation*, Vol.114, No.8 (August 2006), pp. 357-358.
- Rochitte, CE.; Oliveira, PF.; Andrade, JM.; Ianni, BM.; Parga, JR.; Avila, LF.; Kalil-Filho, R.; Mady, C.; Meneghetti, JC.; Lima, JA. & Ramires, JA. (2005). Myocardial delayed enhancement by magnetic resonance imaging in patients with Chagas' disease: a marker of disease severity. *J Am Coll Cardiol*, Vol.46, No.8, (Oktober 2005), pp. 1553-1558.
- Rochitte, CE.; Nacif, MS.; de Oliveira Junior, AC.; Siqueira-Batista, R.; Marchiori, E.; Uellendahl, M. & de Lourdes HM. (2007). Cardiac magnetic resonance in Chagas' disease. *Artif Organs*, Vol.31, No.4 (April 2007) pp. 259-267.
- Rochitte, CE.; Olivera, PF. & Joalbo M. (2003). Chagas disease is characterised by specific pattern and location of myocardial delayed enhancement MRI. *J Cardiovasc Magn Reson*, Vol. 5 (2003), pp. 113
- Roes, SD.; Borleffs, C.; van der Geest, RJ.; Westenberg, JJM.; Marsan, NA.; Kaandorp, TAM.; Reiber, JHC.; Zeppenfeld, K.; Lamb, HJ. & de Roos. (2009). Infarct Tissue Heterogeneity Assessed With Contrast-Enhanced MRI Predicts Spontaneous Ventricular Arrhythmia in Patients With Ischemic Cardiomyopathy and Implantable Cardioverter-Defibrillator. *Circulation: Cardiovascular imaging*, Vol.2, No.3, (2009), pp.183
- Thygesen, K.; Alpert, JS. & White HD. (2007). Universal definition of myocardial infarction. *Eur Heart J*, Vol.28, No.20, (Oktober 2007), pp. 2525-2538.
- Rubinshtein, R.; Glockner, JF.; Ommen, SR.; Araoz, PA.; Ackerman, MJ.; Sorajja, P.; Bos, JM.; Tajik. AJ.; Valeti, US.; Nishimura, A. & Gersh BJ. (2010). Characteristics and clinical significance of late gadolinium enhancement by contrast-enhanced magnetic resonance imaging in patients with hypertrophic cardiomyopathy. *Circ Heart Fail*, Vol.3, No.1, (January 2010), pp. 51-58.
- Sharkey, SW.; Lesser, JR.; Maron, MS. & Maron BJ. (2011). Why not just call it tako-tsubo cardiomyopathy: a discussion of nomenclature. *J Am Coll Cardiol*, Vol.57, No.13 (March 2011), pp. 1496-1497.
- Shimada, T.; Shimada, K.; Sakane, T.; Ochiai, K.; Tsukihashi, H.; Fukui, M.; Inoue, S.; Katoh, H.; Murakami, Y.; Ishibashi, Y. & Maruyama, R. (2001). Diagnosis of cardiac sarcoidosis and evaluation of the effects of steroid therapy by gadolinium-DTPA-enhanced magnetic resonance imaging. *Am J Med*, Vol.110, No.7 (May 2001), pp. 520-527.
- Sievers, B.; Moon, JC. & Pennell DJ. (2002). Images in cardiovascular Medicine. Magnetic resonance contrast enhancement of iatrogenic septal myocardial infarction in hypertrophic cardiomyopathy. *Circulation*, Vol. 105, No.8, (February 2002), pp. 1018.
- Stensaeth, KH.; Fossum, E.; Hoffmann, P.; Mangschau, A.; Skretteberg, PT. & Klow, NE. (2011). Takotsubo cardiomyopathy in acute coronary syndrome; clinical features and contribution of cardiac magnetic resonance during the acute and convalescent phase. *Scand Cardiovasc J*, Vol.45, No.2, (April 2011), pp. 77-85.
- Stoel, MG.; von Birgelen, C. & Zijlstra F. (2009). Aspiration of embolized thrombus during primary percutaneous coronary intervention. *Catheter Cardiovasc Interv*, Vol.73, No.6 (May 2009), pp. 781-786.
- Van der Zwaan, HB.; Stoel, MG.; Roos-Hesselink, JW.; Veen, G.; Boersma, E. & von Birgelen C. (2010). Early versus late ST-segment resolution and clinical outcomes after percutaneous coronary intervention for acute myocardial infarction. *Neth Heart J*, Vol.18, No.9 (September 2010), pp. 416-422.

- Vogel-Claussen, J.; Rochitte, CE.; Wu, KC.; Kamel, IR.; Foo, TK, Lima, JA.; Bluemke, DA. (2006). Delayed enhancement MR imaging: utility in myocardial assessment. *Radiographics*, Vol.26, No.3 (May 2006) pp. 795-810.
- Vohringer, M.; Mahrholdt, H.; Yilmaz, A. & Sechtem U. (2007) Significance of late gadolinium enhancement in cardiovascular magnetic resonance imaging (CMR). *Herz* Vol. 32, No.2, (March 2007), pp. 129-137.
- Wassmuth, R.; Lentzsch, S.; Erdbruegger, U.; Schulz-Menger, J.; Doerken, B.; Dietz, R. & Friedrich MG. (2001). Subclinical cardiotoxic effects of anthracyclines as assessed by magnetic resonance imaging-a pilot study. *Am Heart J*, Vol.141, No.6, (June 2001), pp. 1007-1013.
- Weinsaft, JW.; Klem, I. & Judd RM. (2007). MRI for the assessment of myocardial viability. *Cardiol Clin*, Vol.25, No.1 (February 2007), pp. 35-56.
- Wu, CF.; Chuang, WP.; Li, AH. & Hsiao CH. (2009). Cardiac magnetic resonance imaging in sunitinib malate-related cardiomyopathy: no late gadolinium enhancement. *J Chin Med Assoc*, Vol.72, No.6, (June 2009), pp. 323-327.
- Wynne, J. & Braunwald E. (2005). Restrictive and infiltrative cardiomyopathies. In: Zipes, DP.; Libby, P.; Bonow, RO. & Braunwald E, editors. *Braunwald's heart disease: a textbook of cardiovascular medicine*. p. 1682-1692. Elsevier Saunders, Philadelphia, Pennsylvania.
- Yasu, T.; Tone, K.; Kubo, N. & Saito M. (2009). Transient mid-ventricular ballooning cardiomyopathy: a new entity of Takotsubo cardiomyopathy. *Int J Cardiol*, Vol.110, No.1, (June 2006), pp. 100-101.
- Yeh, ET. & Bickford CL. (2009). Cardiovascular complications of cancer therapy: incidence, pathogenesis, diagnosis, and management. *J Am Coll Cardiol*, Vol.53, No.24, (June 2009), pp. 2231-2247.
- Yelgec, NS.; Dymarkowski, S.; Ganame, J. & Bogaert J. (2007). Value of MRI in patients with a clinical suspicion of acute myocarditis. *Eur Radiol*, Vol.17, No.9, (September 2007), pp. 2211-2217.
- Yilmaz, A.; Gdynia, HJ.; Baccouche, H.; Mahrholdt, H.; Meinhardt, G.; Basso, C.; Thiene, G.; Sperfeld, AD.; Ludolph, AC. & Sechtem U. (2008). Cardiac involvement in patients with Becker muscular dystrophy: new diagnostic and pathophysiological insights by a CMR approach. *J Cardiovasc Magn Reson*, Vol.10, No.1, (2008), pp. 50.
- Yilmaz, A.; Kindermann, I.; Kindermann, M.; Mahfoud, F.; Ukena, C.; Athanasiadis, A.; Hill, S.; Mahrholdt, H.; Voehringer, M.; Schieber, M.; Klingel, K.; Kandolf, R.; Bohm, M. & Sechtem U. (2010). Comparative evaluation of left and right ventricular endomyocardial biopsy: differences in complication rate and diagnostic performance. *Circulation*, Vol.122, No.9, (August 2010), pp. 900-909.
- Yokokawa, M.; Tada, H.; Koyama, K.; Ino, T.; Hiramatsu, S.; Kaseno, K.; Naito, S.; Oshima, S. & Taniguchi, K. (2009). The characteristics and distribution of the scar tissue predict ventricular tachycardia in patients with advanced heart failure. *Pacing Clin Electrophysiol*, Vol.32, No.3, (March 2009), pp. 314-322.
- Yokokawa, M.; Tada, H.; Koyama, K.; Naito, S.; Oshima, S. & Taniguchi, K. (2009). Nontransmural scar detected by magnetic resonance imaging and origin of ventricular tachycardia in structural heart disease. *Pacing Clin Electrophysiol*, Vol.32, No1. (March 2009), pp. 52-56.
- Zagrosek, A.; Wassmuth, R.; bdel-Aty, H.; Rudolph, A.; Dietz, R. & Schulz-Menger, J. (2008). Relation between myocardial edema and myocardial mass during the acute and convalescent phase of myocarditis--a CMR study. *J Cardiovasc Magn Reson*, Vol.10, No.1, (2008), pp. 19.



Cardiomyopathies - From Basic Research to Clinical Management

Edited by Prof. Josef Veselka

ISBN 978-953-307-834-2

Hard cover, 800 pages

Publisher InTech

Published online 15, February, 2012

Published in print edition February, 2012

Cardiomyopathy means "heart (cardio) muscle (myo) disease (pathy)". Currently, cardiomyopathies are defined as myocardial disorders in which the heart muscle is structurally and/or functionally abnormal in the absence of a coronary artery disease, hypertension, valvular heart disease or congenital heart disease sufficient to cause the observed myocardial abnormalities. This book provides a comprehensive, state-of-the-art review of the current knowledge of cardiomyopathies. Instead of following the classic interdisciplinary division, the entire cardiovascular system is presented as a functional unity, and the contributors explore pathophysiological mechanisms from different perspectives, including genetics, molecular biology, electrophysiology, invasive and non-invasive cardiology, imaging methods and surgery. In order to provide a balanced medical view, this book was edited by a clinical cardiologist.

How to reference

In order to correctly reference this scholarly work, feel free to copy and paste the following:

Marlon A.G.M. Olimulder, Michel A. Galjee, Jan van Es, Lodewijk J. Wagenaar and Clemens von Birgelen (2012). The Use of Contrast-Enhancement Cardiovascular Magnetic Resonance Imaging in Cardiomyopathies, *Cardiomyopathies - From Basic Research to Clinical Management*, Prof. Josef Veselka (Ed.), ISBN: 978-953-307-834-2, InTech, Available from: <http://www.intechopen.com/books/cardiomyopathies-from-basic-research-to-clinical-management/the-use-of-contrast-enhancement-cardiovascular-magnetic-resonance-imaging-in-cardiomyopathies>

INTECH

open science | open minds

InTech Europe

University Campus STeP Ri

Slavka Krautzeka 83/A

51000 Rijeka, Croatia

Phone: +385 (51) 770 447

Fax: +385 (51) 686 166

www.intechopen.com

InTech China

Unit 405, Office Block, Hotel Equatorial Shanghai

No.65, Yan An Road (West), Shanghai, 200040, China

中国上海市延安西路65号上海国际贵都大饭店办公楼405单元

Phone: +86-21-62489820

Fax: +86-21-62489821

© 2012 The Author(s). Licensee IntechOpen. This is an open access article distributed under the terms of the [Creative Commons Attribution 3.0 License](#), which permits unrestricted use, distribution, and reproduction in any medium, provided the original work is properly cited.